Complete 3D Surface Reconstruction from Unstructured Point Cloud

Seok-Il Kim*, Rixie Li
School of Aerospace and Mechanical Engineering, Hankuk Aviation University, Goyang-si, Gyeonggi-do 412-791, Korea

In this study, a complete 3D surface reconstruction method is proposed based on the concept that the vertices of surface model can be completely matched to the unstructured point cloud. In order to generate the initial mesh model from the point cloud, the mesh subdivision of bounding box and shrink-wrapping algorithm are introduced. The control mesh model for well representing the topology of point cloud is derived from the initial mesh model by using the mesh simplification technique based on the original QEM algorithm, and the parametric surface model for approximately representing the geometry of point cloud is derived by applying the local subdivision surface fitting scheme on the control mesh model. And, to reconstruct the complete matching surface model, the insertion of isolated points on the parametric surface model and the mesh optimization are carried out. Especially, the fast 3D surface reconstruction is realized by introducing the voxel-based nearest-point search algorithm, and the simulation results reveal the availability of the proposed surface reconstruction method.

Key Words : Reverse Engineering, Surface Reconstruction, Point Cloud, Complete Matching, Shrink Wrapping

1. Introduction

The reverse engineering means to generate engineering models from real objects. Especially, the shape reverse engineering means to generate shape models available in CAD/CAM systems from point clouds or multiple images (Cho and Samuel, 2003; Mülayim et al., 2003) measured from real parts. The application examples of this shape reverse engineering can be found in the duplication of real parts without design drawing, the development of new products through the analysis and improvement of existing parts, the generation of CAD models from mock-ups manufactured by style designers at the initial product development stage, and so on.

The shape reverse engineering procedures are basically consisted of the measurement, shape reconstruction and CAD model generation of the parts. The recent remarkable improvement of the optical and image processing technologies has produced the various forms of the high-efficient 3D measurement equipment. As a result, the amounts of measurement information have remarkably increased with the reduction of measuring time. Therefore the various methods for rapidly reconstructing the more accurate and reliable 3D surface or CAD model from the point cloud, become presented.

Many studies related to the 3D surface reconstruction from the point cloud are carried out based on the Delaunay triangulation method. Gopi et al. (2000) derived the 2D Delaunay triangulation as projecting the neighborhood of each sample point on a tangent plane, and reconstructed the 3D surface as mapping the result into the 3D

* Corresponding Author,
E-mail : sikim@hau.ac.kr
TEL : +82-2-300-0176; **FAX** : +82-2-3158-4231
School of Aerospace and Mechanical Engineering, Hankuk Aviation University, Goyang-si, Gyeonggi-do 412-791, Korea. (Manuscript **Received** January 13, 2006; **Revised** September 4, 2006)

space. Hoppe et al.(1992) calculated a tangent plane at each sample point as using its k-nearest neighbors and tried to reconstruct the 3D surface as using the marching cubes algorithm and the signed distance of the sample point nearest from the tangent plane. Bernardini et al.(1999) proposed the ball pivoting algorithm that rolls a ball over the point cloud, based on the normal to the surface at each point. And Boissonnant (1984) estimated a tangent plane around the initial border edge in the triangulated reconstruction and proposed the reconstruction method that the sample point maximizing the angle between both vertices and the k-nearest neighbors projected onto the tangent plane becomes a vertex of surface triangle. But these approaches based on the Delaunay triangulation method has the demerits that, when the number of sample points is increased, the reconstruction time is rapidly increased and the error in the 3D surface reconstruction may be caused.

Also Lee et al.(2000) proposed the displaced subdivision surface that can represent a detailed model as a scalar displacement map over a smooth subdivision surface. The control mesh model is obtained via the mesh simplification process of the initial mesh model, and the 3D surface reconstruction is realized by repeatedly performing the subdivision, displacement and resampling processes on the control mesh model. Jeong and Kim (2002) introduced an approach for reconstruction of a displaced subdivision surface directly from the point cloud. The coarse base mesh is created from the bounding box containing the point cloud, and the initial coarse control mesh is constructed by the shrink wrapping approach. And the fine surface is sampled directly from the point cloud along the each limit vertex normal without any connectivity information of the given points. But, because these 3D surface reconstruction methods perform only the surface approximation to the point cloud, there is the error between the reconstructed surface and the point cloud.

Therefore, in this study, we propose a complete 3D surface reconstruction method which the 3D surface reconstruction time is short and the reconstructed surface model represents well the geometry and topology information of the unstructured point cloud without modeling error because the vertices of the reconstructed surface model are one-to-one corresponding to the sample points given as the point cloud. Firstly, the initial mesh model describing roughly the point cloud is derived by repeatedly performing the mesh subdivision and shrink-wrapping processes (Leif et al., 1999) on the rectangular parallelepiped bounding box containing the point cloud. The mesh simplification process using the vertex based QEM (Quadric Error Metrics) algorithm (Michael and Paul, 1997) is applied to generate the control mesh model from the initial mesh model. The control mesh model means the mesh model that can represent well the topology information of the point cloud and has the minimum difference between the number of the sample points and the number of mesh vertices obtaining via the additional mesh subdivision process. And the parametric surface model (Suzuki et al., 1999) representing very approximately the point shape is obtained by applying the local subdivision surface fitting method (Taubin, 1995) to the control mesh model. Finally, to reconstruct the complete matching surface model of which vertices coincide completely with the sample points, the insertion of isolated points on the parametric surface model and the mesh optimization are carried out. Also, to greatly reduce the 3D surface reconstruction time as solving the problem that the increase in the number of the sample points leads to a drastic increase in the search time for the neighbor points, we suggest the voxel based nearest point search method of which the search time is very short because of managing only a few sample points in the local infinitesimal spaces. Especially, the usefulness of the complete 3D surface reconstruction method proposed in this study is demonstrated via the reconstruction results of the significant examples such as the golf club head model and the ball joint model.

2. Complete 3D Surface Reconstruction

2.1 Voxel based nearest point search

In the 3D surface reconstruction process, it is

necessary to establish the relationships between the sample points and the vertices and meshes of shape model. Especially, because the increase in the number of the sample points leads to a drastic increase in the search time for the neighbor points, the search efficiency of the nearest point search method is very important to reduce the 3D surface reconstruction time. Therefore we suggest the voxel based nearest point search method of which the search time is very short because of managing only a few sample points in the local infinitesimal spaces.

First of all, it needs to obtain the rectangular parallelepiped bounding box from the coordinates of the sample points given as the point cloud. And, after subdividing the bounding box into the uniform voxels, it is required to allocate each sample point and each vertex of shape models to the voxel containing the points. Let (p_x, p_y, p_z) be the coordinate of the sample point, let (v_x, v_y, v_z) be the coordinate of the vertex of shape model, let $(x_{\min}, y_{\min}, z_{\min})$ the coordinate of the reference vertex of bounding box, and let δ be the size of voxel. Then, as shown in Fig. 1, the index of the voxel containing the sample point or the vertex can be expressed as follows:

$$i=\frac{p_x-x_{\min}}{\delta},\ j=\frac{p_y-y_{\min}}{\delta},\ k=\frac{p_z-z_{\min}}{\delta} \quad (1)$$

$$i=\frac{v_x-x_{\min}}{\delta},\ j=\frac{v_y-y_{\min}}{\delta},\ k=\frac{v_z-z_{\min}}{\delta} \quad (2)$$

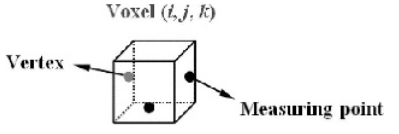

Fig. 1 Voxel with measuring points and/or vertices

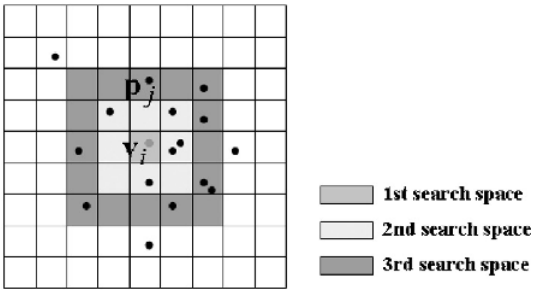

Fig. 2 Search of nearest point

Figure 2 shows an example of searching the sample point nearest from the vertex of shape model. Basically, the distances between the vertex and the sample points are calculated within the first search space which means the single voxel containing the vertex, and also within the second search spaces which mean the 26 voxels of the exterior of the first search space. The sample point with the shortest distance becomes the nearest sample point. In the case that the nearest sample point does not exist within the first and second search spaces, the nearest sample point is searched via the expansion of the search space such as the third search space, the fourth search space, and so on. Therefore, because this voxel based nearest point search method finds the nearest point among some sample points within the limited local spaces, it has the merit that the nearest point search time is very short.

2.2 Generation of initial mesh model

In this study, to reconstruct the 3D surface from the unstructured point cloud, the initial mesh model describing roughly the point cloud is generated by repeatedly applying the mesh subdivision and shrink-wrapping processes to the rectangular parallelepiped bounding box containing the point cloud. Figure 3(a) shows the initial bounding box which contains the point cloud and consists of the 12 triangular meshes and the 8 vertices.

In order to create the initial mesh model with as many vertices as possible under the restriction that the number of vertices of the initial mesh model has to be less than or equal to the number of the sample points, it is required to subdivide

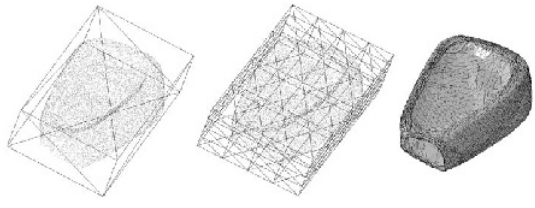

(a) (b) (c)

Fig. 3 Generation of initial mesh model by subdivision and shrink-wrapping: (a) initial bounding box, (b) subdivided bounding box, (c) initial mesh model

the triangular meshes of the initial bounding box. Because the subdivision process of the triangular mesh, as shown in Fig. 3(b), is based on the concept which assigns the middle point of each edge for the new vertex, the number of the triangular meshes is increased 4 times whenever the mesh subdivision process is carried out. The relation between the numbers of the triangular meshes and the vertices is given as Eq. (3). Therefore the maximum iteration number of the subdivision process, which has to be applied to the triangular meshes of the initial bounding box, can be determined from the number of the sample points.

$$N_{triangle}=2N_{vertex}-4 \tag{3}$$

where $N_{triangle}$ is the number of the triangular meshes and N_{vertex} is the number of the vertices.

And, to obtain the initial mesh model in Fig. 3(c) from the subdivided bounding box in Fig. 3(b), it is necessary to introduce the projection and smoothing operations of the shrink-wrapping algorithm.

The projection force $\mathbf{f}_{v_i}$ in Fig. 4 is defined as the vector between the sample point $\mathbf{p}_j$ and the vertex $\mathbf{v}_i$ of the mesh as expressed in Eq. (4), and is applied to all the vertices of each triangular mesh in the projection operation.

$$\mathbf{f}_{v_i}=\mathbf{p}_j-\mathbf{v}_i \tag{4}$$

After searching the nearest sample points for all the vertices of each triangular mesh, the shape model $\mathbf{M}_b$, which consists of the vertices of the triangular meshes more adjacent to the sample points, can be obtained as Eq. (5) via the projection force $\mathbf{f}_{v_i}$ in Eq. (4) and the projection speed parameter $\xi\in[0,1]$.

$$\mathbf{M}_b=\sum_i(\mathbf{v}_i+\xi\mathbf{f}_{v_i}) \tag{5}$$

In the case that a vertex of the subdivided bounding box shares the same sample point as the nearest point with the other vertices, if the projection speed parameter ξ is 1.0, the distorted shape model is obtained because the relevant vertices have the same coordinates. Therefore, in order to prevent this distortion in the generation process of the initial mesh model, the projection speed parameter ξ has to be less than 1.0. In this study, we identify empirically the fact that the best projection result can be derived regardless of the shape when the projection speed parameter ξ is 0.85.

The smoothing operation of the shrink-wrapping algorithm is a relaxation operation for achieving the uniformly distributed meshes. The Laplacian vector $\mathbf{L}(\mathbf{v}_i)$ (Hoppe et al.,1992) in Eq. (6) means the average of the edge vectors sharing a vertex $\mathbf{v}_i$. Then, as shown in Fig. 5, the tangential vector $\mathbf{L}_t(\mathbf{v}_i)$ at the vertex can be calculated as Eq. (7) by using the Laplacian vector $\mathbf{L}$ and the normal vector $\mathbf{n}$ at the vertex.

$$\mathbf{L}(\mathbf{v}_i)=\frac{1}{K_{v_i}}\sum_{v_k\in N_{nb}(v_i)}(\mathbf{v}_k-\mathbf{v}_i) \tag{6}$$

$$\mathbf{L}_t(\mathbf{v}_i)=\mathbf{L}(\mathbf{v}_i)-\{\mathbf{L}(\mathbf{v}_i)\cdot\mathbf{n}\}\mathbf{n} \tag{7}$$

And the smoothed shape model is obtained based on the tangential vector $\mathbf{L}_t(\mathbf{v}_i)$ and the relaxation speed parameter η for controlling the convergence speed of the smoothing operation as follows:

$$\mathbf{M}_b^*=\mathbf{M}_b+\sum_i\eta\mathbf{L}_t(\mathbf{v}_i) \tag{8}$$

As the relaxation speed parameter η becomes larger, the shape model can be more uniform. However, it is difficult to depict the regions that the more detailed descriptions are required because of the extreme shape variation. Therefore, assigning the appropriate value to the relaxation

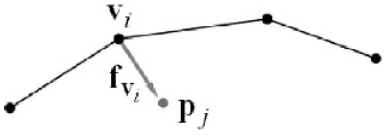

Fig. 4 Projection force

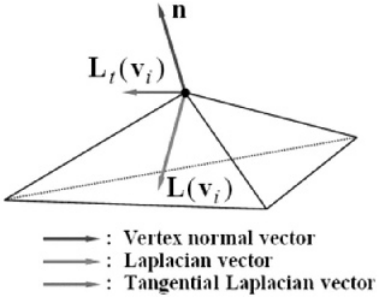

Fig. 5 Normal and Laplacian vectors

speed parameter η is important in the 3D surface reconstruction. In this study, the relaxation speed parameter η is empirically determined as 0.2.

2.3 Generation of control mesh model

The initial mesh model depicts roughly the geometry information of the point cloud, but not the topology information of the point cloud. And the control mesh model means the mesh model that can represent well the topology information of the point cloud and has the minimum difference between the number of the sample points and the number of mesh vertices obtaining via the additional mesh subdivision process. In order to generate the control mesh model from the initial mesh model, the simplification process of the mesh model is required. Especially, because the control mesh model has significant influence on the finally reconstructed surface, the generation of the optimal control mesh model is important in the 3D surface reconstruction. Therefore, in this study, the mesh simplification process using the vertex based QEM algorithm is introduced to generate from the initial mesh model in Fig. 3(c) to the optimal control mesh model in Fig. 6.

The mesh simplification process using the vertex based QEM algorithm can be divided into the vertex pair contraction and the error quadric estimation as follows:

(1) The plane equations of the triangular meshes sharing a vertex are expressed as shown in Eq. (9).

$$\mathbf{P}=[a\ b\ c\ d]^T \tag{9}$$

where $ax+by+cz+d=0$ and $a^2+b^2+c^2=1$.

(2) The fundamental error quadric $\mathbf{K}_\mathrm{p}$ is calculate based on the plane equation $\mathbf{P}$ of the triangular mesh as below:

$$\mathbf{K}_\mathrm{p}=\mathbf{P}\mathbf{P}^T=\begin{bmatrix} a^2 & ab & ac & ad \\ ab & b^2 & bc & bd \\ ac & bc & c^2 & cd \\ ad & bd & cd & d^2 \end{bmatrix} \tag{10}$$

(3) The error quadric $\mathbf{Q}$ for two vertices $\mathbf{v}_1$ and $\mathbf{v}_2$ of each edge is calculated from the fundamental error quadric $\mathbf{K}_\mathrm{p}$ as shown in Eq. (11).

$$\mathbf{Q}_{\mathrm{v}_i}=\sum_{\mathrm{P}\in Plane(\mathrm{v}_i)}\mathbf{K}_\mathrm{p} \tag{11}$$

(4) After calculating the contraction cost C_e in Eq. (12) for all the edges, the vertex $\bar{\mathbf{v}}$ of the contraction target with the least contraction cost is investigated. And the corresponding edge is contracted by merging two vertices $\mathbf{v}_1$ and $\mathbf{v}_2$ into the vertex $\bar{\mathbf{v}}$ as shown in Fig. 7.

$$C_e=\bar{\mathbf{v}}^T(\mathbf{Q}_{\mathrm{v}_1}+\mathbf{Q}_{\mathrm{v}_2})\,\bar{\mathbf{v}} \tag{12}$$

(5) The above processes from the step (1) to the step (4) are repeated until the satisfactory control mesh model is obtained.

2.4 Generation of parametric surface model

The parametric surface model approximately describing the point cloud is necessary to realize the complete 3D surface reconstruction. Therefore, in this study, the parametric surface model is generated by repeatedly applying the local subdivision surface fitting method to the control mesh model.

In the local subdivision surface fitting method, the attraction force $\mathbf{r}_i$, which is needed to move the vertex $\mathbf{v}_i$ shared by the K_{v_i} edges to the nearest sample point $\mathbf{p}^*$, is defined as Eq. (13) by the vector difference between the vertex $\mathbf{v}_i$ and the nearest sample point $\mathbf{p}^*$ and the vector difference between the vertex $\mathbf{v}_i$ and the vertex $\mathbf{v}_j$ sharing the edge with the vertex $\mathbf{v}_i$.

$$\mathbf{r}_i=(\mathbf{p}^*-\mathbf{v}_i)-\chi_i\sum_{j\in i}(\mathbf{v}_j-\mathbf{v}_i) \tag{13}$$

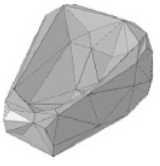

Fig. 6 Control mesh model

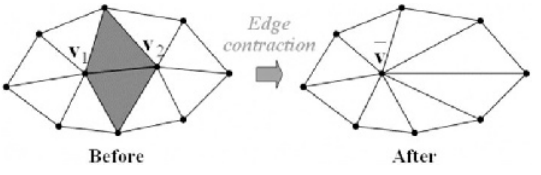

Fig. 7 Edge contraction

where β and χ_i are given as follows:

$$\beta=\begin{cases}\dfrac{3}{16} & (K_{\mathrm{v}_i}=3)\\ \dfrac{1}{K_{\mathrm{v}_i}}\left\{\dfrac{5}{8}-\left(\dfrac{3}{8}+\dfrac{1}{4}\cos\dfrac{2\pi}{K_{\mathrm{v}_i}}\right)^2\right\} & (K_{\mathrm{v}_i}>3)\end{cases}$$

$$\chi_i=\left(\frac{3}{8\beta}+K_{\mathrm{v}_i}\right)^{-1}$$

Especially, if the movement of the vertex $\mathbf{v}_i$ is given as presented in Eq. (14) by the multiplication of the acceleration factor $\lambda\in[0,1]$ and the attraction force $\mathbf{r}_i$, the vertex $\mathbf{v}_i^*$ more adjacent to the nearest sample point $\mathbf{p}^*$ is obtained as shown in Fig. 8. And, by applying this process to all the vertices of the subdivided control mesh model, the parametric surface model such as Fig. 9 can be realized.

$$\mathbf{v}_i^*=\mathbf{v}_i+\lambda\mathbf{r}_i \tag{14}$$

2.5 Generation of complete matching surface model

In this study, we propose a complete surface matching method based on the shrink-wrapping algorithm, which the modeling error of the shape model becomes basically zero because all vertices of the shape model have a one-to-one correspondence with the sample points and both the coordinates coincide with each other.

Firstly, the projection speed parameter ξ in Eq. (5) and the relaxation speed parameter η in Eq. (8) are respectively given as 1.0 and 0.0 from the conditions that all the vertices of the parametric surface model have to coincide with the nearest sample points, and the shrink-wrapping algorithm is applied to the parametric surface model. In this case, because some vertices of the parametric surface model may share the same sample point as the nearest sample point, the abnormal triangular meshes that 2 or more vertices have the identical coordinate can be formed. Therefore, it is necessary to search and eliminate the abnormal triangular meshes.

As a result of eliminating the abnormal triangular meshes, some sample points do not coincide with the vertices of the parametric surface model and are isolated. And, to generate the complete matching surface model, this isolated sample points have to be inserted into the triangular meshes that the distances between the sample points and the foot of perpendicular become minimized. Figure 10 presents the concept that the isolated sample points are inserted into the triangular meshes and are converted to the new vertices of the shape model via the mesh subdivision process. Also, it shows that the triangular meshes become more reasonable via the mesh regulation process using the edge swapping method based on the Max-Min edge criterion.

The insertion process of the isolated sample points, the mesh subdivision process and the mesh regulation process are repeatedly performed until the isolated sample points do not exist. Figure 11 shows the initial complete matching surface model

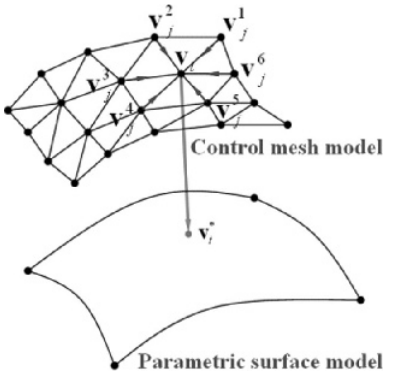

Fig. 8 Surface fitting of vertex $\mathbf{v}_i$

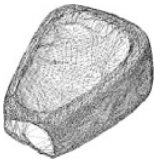

Fig. 9 Parametric surface model

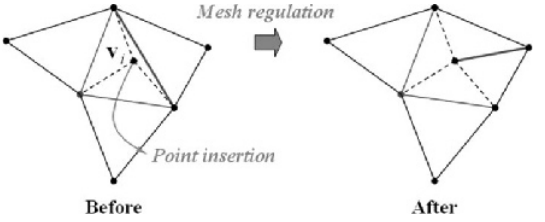

Fig. 10 Point insertion and mesh regulation

that is generated by applying repeatedly (3 times) these processes to the parametric surface model in Fig. 9.

The initial complete matching surface model consists of only the uniform meshes regardless of the geometry and topology information of the point cloud. Therefore, to consider closely the geometry and topology information of the point cloud, the mesh optimization process is required. In this study, as in the above mentioned mesh simplification process using the vertex based QEM algorithm, the contraction costs in Eq. (12) are estimated for the original edge and the virtual diagonal transpose edge of the initial complete matching surface model as shown in Fig. 12. And the mesh optimization method, which the meshes are regenerated by the edge with the smaller contraction cost, is proposed. Figure 13 shows the optimized complete matching surface model that is finally reconstructed as introducing this mesh optimization method.

Fig. 11 Initial complete matching surface model

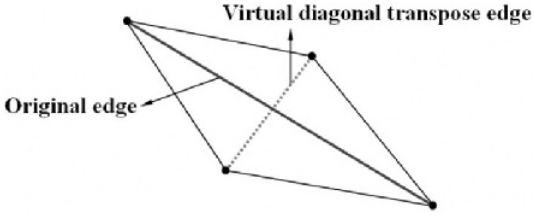

Fig. 12 Original and virtual diagonal transpose edges

Fig. 13 Optimized complete matching surface model

3. Examples and Discussion

In this study, the special program for realizing the complete 3D surface reconstruction from the unstructured point cloud is developed based on the 2.8 GHz Pentium IV computer with 512MB RAM, Visual C^{++}6.0 and OpenGL library. Figure 14 shows the framework of the complete 3D surface reconstruction program, and Figure 15 presents all the complete 3D surface reconstruction processes that generate sequentially the bounding box, the initial mesh model, the control mesh model, the parametric surface model, the initial complete matching surface model and the optimized complete matching surface model from the point cloud.

The golf club head model shown in Fig. 13 is reconstructed from the point cloud consisted of the 12,321 sample points, and the number of vertices and the process time in each surface recon-

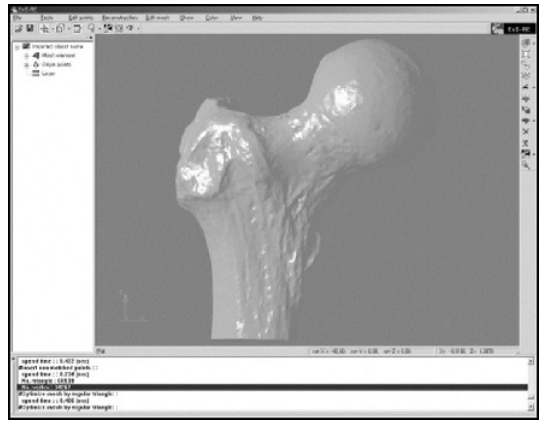

Fig. 14 3D surface reconstruction program

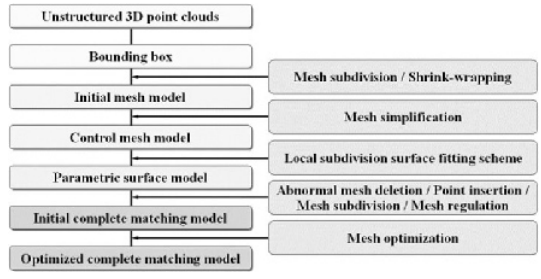

Fig. 15 3D surface reconstruction process

struction process are presented in Table 1. The number of vertices related to the golf club head model is 1,538 in the initial mesh model, 771 in the control mesh model, 12,306 in parametric surface model, and 12,321 in the initial and optimized complete matching surface models. And the total process time related to the golf club head model is 4.892 sec which consists of 0.157 sec in the initial mesh model, 0.188 sec in the control mesh model, 0.516 sec in the parametric surface model, 3.031 sec in the initial complete matching surface model, and 1.000 sec in the optimized complete matching surface model.

Table 1 3D surface reconstruction of golf head

Model	No. of vertices	Process time
Initial mesh model	1,538	0.157 sec
Control mesh model	771	0.188 sec
Parametric surface model	12,306	0.516 sec
Initial complete matching surface model	12,321	3.031 sec
Optimized complete matching surface model	12,321	1.000 sec
Total	—	4.892 sec

Table 2 3D surface reconstruction of ball joint

Model	No. of vertices	Process time
Initial mesh model	6,146	0.767 sec
Control mesh model	2,144	3.422 sec
Parametric surface model	34,274	2.968 sec
Initial complete matching surface model	34,267	5.869 sec
Optimized complete matching surface model	34,267	2.516 sec
Total	—	15.542 sec

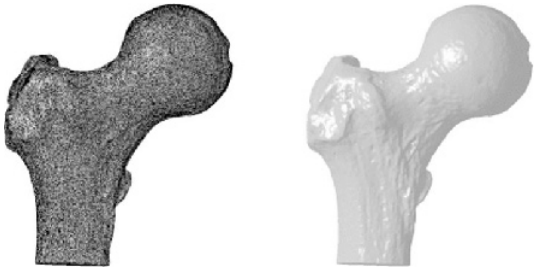

Fig. 16 3D surface reconstruction of ball joint model

Also, Figure 16 shows the ball joint model that is reconstructed from the point cloud consisted of the 34,267 sample points, and Table 2 presents the number of vertices and the process time in each surface reconstruction process. The number of vertices related to the ball joint model is 6,146 in the initial mesh model, 2,144 in the control mesh model, 34,274 in parametric surface model, and 34,267 in the initial and optimized complete matching surface models. And the total process time related to the ball joint model is 15.542 sec which consists of 0.767 sec in the initial mesh model, 3.422 sec in the control mesh model, 2.968 sec in the parametric surface model, 5.869 sec in the initial complete matching surface model, and 2.516 sec in the optimized complete matching surface model.

As indicated by the above examples, the complete 3D surface reconstruction method proposed in this study has a very short process time, and reveals that all the sample points given as the unstructured point cloud have a one-to-one correspondence with the vertices of the complete matching surface model. And the simulation results show that, because the insertion process of the isolated sample points, the mesh subdivision process and the mesh regulation process require a relatively large amount of calculation, the process time for generating the initial complete matching surface model is longer than the others. Also, as shown in the case of the ball joint model in Fig. 16, it is able to confirm the fact that the model with a complex 3D concave and convex geometry can be precisely and efficiently reconstructed via the proposed surface reconstruction method.

4. Conclusions

In this study, we propose a complete 3D surface reconstruction method which the 3D surface reconstruction time is short and the reconstructed surface model represents well the geometry and topology information of the unstructured point

cloud because the vertices of the reconstructed surface model are one-to-one corresponding to the sample points given as the point cloud. And the simulation results demonstrate the usefulness of the proposed method. The results obtained in this study are summarized as follows :

(1) The initial mesh model describing roughly the point cloud is obtained by repeatedly applying the mesh subdivision and shrink-wrapping processes to the rectangular parallelepiped bounding box containing the point cloud.

(2) The control mesh model, which can represent well the topology information of the point cloud and has the minimum difference between the number of the sample points and the number of mesh vertices obtaining via the additional mesh subdivision process, is generated by applying the mesh simplification process using the vertex based QEM algorithm to the initial mesh model.

(3) The parametric surface model, which approximately describes the point cloud, is derived by repeatedly applying the local subdivision surface fitting method to the control mesh model.

(4) The complete surface matching method based on the shrink-wrapping algorithm and the mesh optimization method are proposed to realize the complete matching surface model of which the vertices coincide completely with the sample points given as the point cloud.

(5) The voxel based nearest point search method, of which the nearest point search time is very short because of managing only a few sample points in the local infinitesimal spaces, is proposed to reduce the surface reconstruction time.

(6) Because the insertion process of the isolated sample points, the mesh subdivision process and the mesh regulation process require a relatively large amount of calculation, the process time for generating the initial complete matching surface model is longer than the others.

References

Bernardini, F., Mittelman, J., Rushmeier, H., Silva, C. and Taubin, G., 1999, "The Ball-Pivoting Algorithm for Surface Reconstruction," *IEEE Transaction on Visualization and Computer Graphics*, Vol. 5, No. 4, pp. 349～359.

Boissonnant, J. D., 1984, "Geometric Structures for Three-Dimensional Shape Reconstruction," *ACM Transactions on Graphics*, Vol. 3, No. 4, pp. 266～289.

Cho, J. H. and Song, Samuel M. H., 2003, "Three-Dimensional Shape Reconstruction from Images by Shape-from-Silhouette Technique and Iterative Triangulation," *KSME International Journal*, Vol. 17, No. 11, pp. 1665～1673.

Gopi, M., Krisnan, S. and Silva, C., 2000, "Surface Reconstruction Based on Lower Dimensional Localized Delaunay Triangulation," *Computer Graphics Forum*, Vol. 19, No. 3, pp. 467～478.

Hoppe. H., DeRose., T., Duchamp, T., McDonald, J. and Stuetzle, W., 1992, "Surface Reconstruction from Unorganized Points," *Proceedings of SIGGRAPH*, pp. 71～78.

Jeong, W. K. and Kim, C. H., 2002, "Direct Reconstruction of Displaced Subdivision Surface from Unorganized Points," *Graphical Models*, Vol. 64, No. 2, pp. 78～93.

Lee, A., Moreton, H. and Hoppe, H., 2000, "Displaced Subdivision Surfaces," *Proceedings of SIGGRAPH*, pp. 85～94.

Leif, P. K., Jens, V., Ulf, L. and Seidel, H. P., 1999, "A Shrink Wrapping Approach to Remeshing Polygonal Surface," *Computer Graphics Forum*, Vol. 18, No. 3, pp. 119～130.

Michael, G. and Paul, S. H., 1997, "Surface Simplification Using Quadric Error Metrics," *Proceedings of SIGGRAPH*, pp. 209～216.

Mülayim, A. Y., Ulaş, Y. and Atalay, V., 2003, "Silhouette-based 3D Model Reconstruction from Multiple Images," *IEEE Trans. on Systems, Man, and Cybernetics — Part B*, Vol. 33, No. 4, pp. 582～591.

Suzuki., H., Takeuchi., S. and Kanai., T., 1999, "Subdivision Surface Fitting to a Range of Points," *Proceedings of SIGGRAPH*, pp. 158～167.

Taubin, G., 1995, "A Signal Processing Approach to Fair Surface Design," *Proceedings of SIGGRAPH*, pp. 351～358.